

Quantification and control of the sulfur $c(2 \times 2)$ superstructure on $\{100\}\langle 100\rangle$ Ni for optimization of YSZ, CeO_2 , and SrTiO_3 seed layer texture

C. Cantoni, D.K. Christen, L. Heatherly, M.M. Kowalewski, F.A. List, A. Goyal, G.W. Ownby, D.M. Zehner, B.W. Kang,^{a)} and D.M. Kroeger
Oak Ridge National Laboratory, Oak Ridge, Tennessee 37831

(Received 4 February 2002; accepted 9 July 2002)

We investigated the influence of a chemisorbed S template with $c(2 \times 2)$ structure on the epitaxial growth of different oxide buffer layers on $\{100\}\langle 100\rangle$ Ni. The sulfur superstructure spontaneously forms on the Ni surface during the texturing anneal as a consequence of segregation. However, depending on the initial S bulk concentration and/or specific annealing conditions, the S layer can cover less than the entire substrate's surface. We show that an incomplete $c(2 \times 2)$ coverage causes degradation of the seed buffer layer texture as compared to the substrate texture. A simple step consisting of an H_2S predeposition anneal can be used to control the superstructure coverage and optimize the seed layer texture.

I. INTRODUCTION

The rolling-assisted biaxially textured substrates (RABiTS) technology is based on the epitaxial growth of an oxide buffer layer that is compatible with high- T_c cuprates on a biaxially textured metal substrate. This process is conceptually complex because it involves the interaction between two surfaces with very different chemical and electronic properties. Despite this complexity, many groups in the past few years have been able to deposit several epitaxial buffer layers directly on a Ni substrate. On the basis of these successful experiments, it seemed natural to assume that the oxide seed layers nucleate on a clean and pure Ni surface that is obtained by a reducing heat treatment prior to deposition.¹⁻³ Once oxidation of the Ni surface is prevented by choosing a seed layer that is thermodynamically more stable than NiO (e.g., CeO_2 or Y_2O_3 -stabilized ZrO_2) and depositing it in reducing conditions for Ni, the lattice match between metal and oxide buffer layer is the main factor influencing epitaxial growth. This picture, however, ultimately proved to be inadequate, particularly after the introduction of a continuous reel-to-reel process for fabricating meters-long buffered tape.⁴ In fact, even a slight irreproducibility in the seed layer texture cannot be tolerated in a continuous process, which is more sensitive to local imperfections than short-sample fabrication processes. Structural defects in the seed layer propagate through the additional buffer layers to the superconducting coating

causing substantial suppression of the critical current. To avoid such inconsistency in the buffer layer texture and optimize J_c , we initiated a careful investigation of the structure and chemistry of the textured $\{100\}\langle 100\rangle$ Ni surface and its effect on seed layer nucleation. This study has revealed the existence of a $c(2 \times 2)$ sulfur superstructure on the textured Ni surface that forms after diffusion and surface segregation of sulfur contained in the metal bulk at a level less than 30 wt ppm. In a previous publication we showed that the S superstructure promotes the epitaxial growth of Y_2O_3 -stabilized ZrO_2 (YSZ) on $\{100\}\langle 100\rangle$ Ni. In contrast, the pulsed laser deposition (PLD) of YSZ on clean Ni surfaces results in a (111) orientation of the seed layer.⁵ In this paper we extend the study of the effect of the $c(2 \times 2)$ superstructure to other commonly used seed layers such as CeO_2 and SrTiO_3 . We also report on a more quantitative analysis of the relationship between superstructure and seed layer texture and present a method that provides control of the sulfur coverage on the metal.

II. PLD SEED LAYERS ON $\{100\}\langle 100\rangle$ NI

CeO_2 seed layers are successfully deposited by vapor deposition techniques like e-beam evaporation, reactive sputtering, and PLD. All these techniques use a background H_2O pressure of about 1×10^{-5} torr and a substrate temperature in the range of 600 to 750 °C. Water dissociation provides enough oxygen in the background to form and stabilize the CeO_2 phase without oxidizing the Ni.⁶ The stability of the Ni surface in the presence of water with a partial pressure in the range of 1×10^{-5} torr

^{a)}Presently at the Pohang Superconductivity Center, Dept. of Physics, Pohang University of Science & Technology, Pohang Kyungbuk, 790-784, Republic of Korea.

was investigated by *in situ* reflection high-energy electron diffraction (RHEED) performed inside the laser molecular beam epitaxy chamber used to fabricate films for this study. It was found that such H_2O partial pressure does not cause any structural modification of the sample surface that can be related to growth of NiO islands or adsorbed O. The documented first stage of Ni oxidation consists of a chemisorbed O layer with $p(2 \times 2)$ structure up to a coverage of 0.25 ML and with subsequent $c(2 \times 2)$ structure up to a coverage of 0.5 ML⁷ [1 ML \equiv (number of surface adsorbate atoms)/(number of surface substrate atoms)]. None of these structures was observed to form as a consequence of water exposure on a clean $\{100\}\langle 100\rangle$ Ni surface at a typical deposition temperature of 600 °C. In this case the clean Ni surface was obtained by depositing a Ni film *in situ* on the textured Ni substrate in ultrahigh vacuum conditions at 600 °C by PLD. In any case, RHEED patterns showed that, when present, the S superstructure that formed after bulk-to-surface segregation was stable at typical CeO_2 deposition conditions.

Figure 1(a) shows a RHEED pattern acquired during the nucleation of CeO_2 on a $\{100\}\langle 100\rangle$ Ni substrate having the $c(2 \times 2)$ -S superstructure shown in Fig. 1(b). The electron beam is directed along the Ni $\langle 100\rangle$. The CeO_2 film was grown at 600 °C in the presence of a water partial pressure of 1.5×10^{-5} torr. The pattern

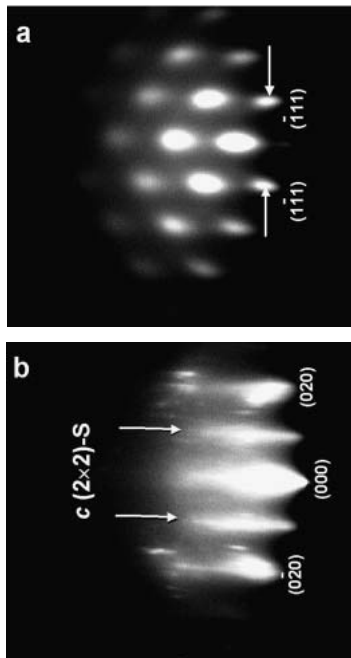


FIG. 1. RHEED pattern obtained at 600 °C during the nucleation of a CeO_2 seed layer on a biaxially textured Ni substrate with a $c(2 \times 2)$ -S surface structure. (a) The electron beam is directed along the Ni $\langle 100\rangle$ and the spacing indicated by the arrows corresponds to the interatomic distance $a_{\text{CeO}_2}\sqrt{2}/2$. (b) Substrate RHEED pattern showing the extra reflections indicating the sulfur $c(2 \times 2)$ superstructure.

shows diffracted spots that correspond to a (002) biaxially textured CeO_2 film viewed along the $\langle 110\rangle$ crystal direction. This is consistent with the general observation that CeO_2 grows with a 45° in-plane rotation with respect to the $\{100\}\langle 100\rangle$ Ni substrate. The presence of spots in the RHEED pattern indicates that the nucleation is occurring by formation of islands, which are tall enough to produce a transmission diffraction pattern. The spacing between the RHEED reflections in Fig. 1(a) provides a rough estimate of the in-plane lattice parameter of the film, which is 5.43 ± 0.05 Å. Figure 2 shows an x-ray diffraction ϕ scan of the (111) peak for the completed CeO_2 film, approximately 400-Å thick. We found that, similarly to what we observed for YSZ,⁵ the deposition of CeO_2 on the $c(2 \times 2)$ -S template consistently produced highly textured (200) films, while deposition on a clean Ni surface always gave rise to (111)-oriented films.

Another oxide that has been used successfully as a seed layer for high temperature superconductor (HTS)-based coated conductors is SrTiO_3 (STO).⁸ Although STO is thermodynamically less stable than bulk NiO, it can be easily grown on Ni at oxygen pressures as low as 1×10^{-9} torr, in conditions at which surface NiO will not form. According to the thermodynamics for the bulk chemical reaction $2\text{Ni} + \text{O}_2 = 2\text{NiO}$, an oxygen pressure in the range of 10^{-9} torr is sufficient to form NiO at a typical deposition temperature of 600 °C. However, surface contributions to the free energy of formation of NiO appear to be significant. Our RHEED experiments have shown that the surface of $\{100\}\langle 100\rangle$ Ni is in fact stable in any oxygen partial pressure as high as 5×10^{-7} torr at a temperature of 600 °C. The ease of growth of STO on Ni can be attributed in part to the stability of the STO crystal structure in presence of oxygen vacancies.⁹

Similarly to CeO_2 and YSZ, STO grows epitaxially on $\{100\}\langle 100\rangle$ Ni only when the $c(2 \times 2)$ -S superstructure is present on the Ni substrate prior to deposition. Figure 3(a) shows the RHEED pattern for a (200) epitaxial STO film grown on the textured Ni substrate. The electron beam is directed along the $\langle 100\rangle$ direction, and the epitaxial relationship between STO and Ni is cube on cube. The corresponding STO (111) pole figure is shown

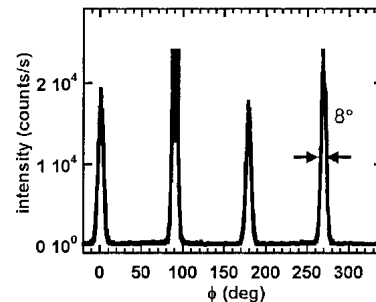
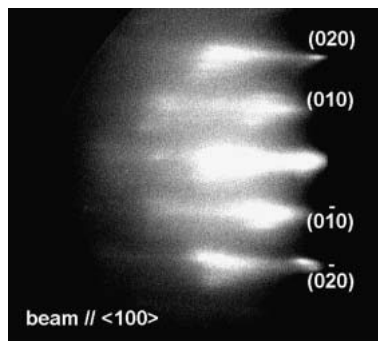


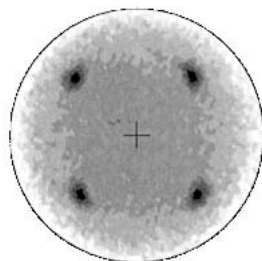
FIG. 2. X-ray diffraction ϕ scan of the (111) peak for a CeO_2 seed layer deposited on the $c(2 \times 2)$ sulfur template chemisorbed on $\{100\}\langle 100\rangle$ Ni.

in Fig. 3(b). The STO films were grown at a substrate temperature of 700 °C. The oxygen pressure was kept in the range 1×10^{-9} – 1×10^{-8} torr during the deposition of a 20–100 Å-thick nucleation layer and then increased to a value of about 1.0×10^{-5} torr. On a clean (1×1) Ni surface, the STO seed layer grows multidomain, with the cube axis remaining parallel to the substrate normal, but with two additional in-plane orientations besides the one with STO $\langle 100\rangle // \text{Ni} \langle 100\rangle$, as shown by the (111) pole figure in Fig. 4.

It is evident that the $c(2 \times 2)$ -S superstructure plays a very important role in the nucleation of an oxide buffer layer on Ni. The physical and chemical properties of a metal surface and their modifications due to chemisorption are certainly very complex. Even more complex are the processes involved in the epitaxial growth of oxides on such surfaces. We proposed that the role played by the S superstructure can be partially explained on the basis of structural and chemical considerations. The S layer behaves like a template that well matches and mimics the arrangement of the oxygen atoms in particular (001) sublattice planes of YSZ, CeO_2 , or STO, as shown in Fig. 5. Sulfur belongs to the VI group and is chemically very similar to oxygen, often exhibiting the same electronic valence. Therefore, it is plausible that during the seed layer deposition the cations easily bond to the S atoms already present on the substrate surface, giving rise to the (001) epitaxial growth of the film, which otherwise would not take place.



(a)



(b)

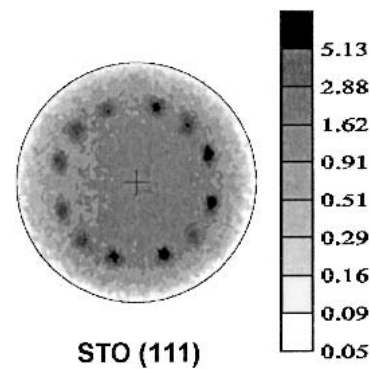
STO (111)

FIG. 3. (a) RHEED pattern of an STO film grown epitaxially on a $\{100\}\langle 100\rangle$ Ni substrate showing the $c(2 \times 2)$ sulfur superstructure. (b) Corresponding (111) logarithmic pole figure of the STO film indicating cube on cube epitaxial relationship with the Ni substrate.

Such structural argument for the effect of the S template on seed layer nucleation is supported by the observation that other oxides with crystal structures very similar to perovskites and fluorites, like LaMnO_3 , and Gd_2O_3 or Y_2O_3 also grow epitaxially on $\{100\}\langle 100\rangle$ Ni only in presence of an intervening $c(2 \times 2)$ -S superstructure.¹⁰

Ironically, the desired structural and chemical properties of RABiT substrates made in the past few years can be attributed, partially, to the involuntary presence of a sufficient S content in the rolled Ni metal.

In cases for which the bulk S content of particular batches of Ni was much lower than 30 wt ppm, the seed layer deposition process produced films with degraded texture or even partially (111) orientation. In those cases, as a recent Auger electron spectroscopy (AES) analysis revealed,⁴ S was depleted in the near-surface layer during



STO (111)

FIG. 4. Pole figure of the (111) reflection in logarithmic scale for an STO film grown on a clean (1×1) -textured Ni surface. Besides the cube-texture peaks, reflections from two additional crystal domains are present.

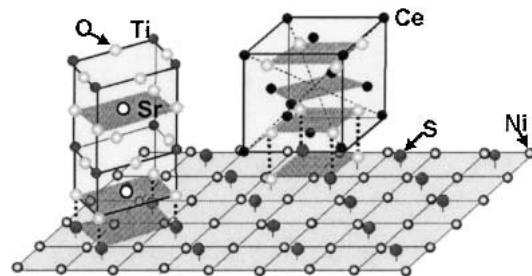


FIG. 5. Schematic model for the nucleation of CeO_2 (or YSZ) and STO on a (001) Ni surface with chemisorbed $c(2 \times 2)$ sulfur superstructure. The dashed lines indicate correspondence between oxygen sites in (001) planes of the seed layer and sulfur sites on the Ni surface. The seed layer cations impinging on the Ni surface bond easily to the sulfur atoms present on the metal surface, promoting the (001) orientation of the growing film. In the STO case, there is a 1:1 correspondence between oxygen atoms in the SrO plane and sulfur atoms on the Ni surface. Therefore, it is plausible that Ti ions initially bond to the S surface atoms to form the first TiO_2 plane of the STO structure. In the CeO_2 case, two of four oxygen ions/unit cell match the sulfur atoms of the $c(2 \times 2)$. During nucleation of CeO_2 , oxygen atoms may fill in the empty fourfold Ni hollows and the Ce cations subsequently bond to the template formed by S and O.

a high-temperature anneal (approximately 1100 °C). This may be the result of the formation and subsequent desorption of SO_2 in the presence of a sufficient partial pressure of oxygen. Sulfur depletion impeded formation of a continuous $c(2 \times 2)$ layer across the entire Ni surfaces, drastically modifying the oxide film nucleation.

III. QUANTIFICATION AND CONTROL OF THE S-SUPERSTRUCTURE

The above-mentioned considerations illustrate a connection between the quality of the seed layer texture and the degree of coverage of the $c(2 \times 2)$ superstructure on Ni. To investigate this aspect, we conducted combined AES and RHEED experiments aimed at quantifying the coverage of the $c(2 \times 2)$ structure on different Ni samples. During Auger spectroscopy experiments, depending on the material under test and the beam energy, Auger electrons escape and are detected from a layer 5–10-Å deep below the atomistic surface. Therefore, the S concentration as deduced from AES can differ from the actual atomic concentration of the top monolayer of the surface (i) because of the uncertainty related to the measurement itself and (ii) because, after segregation, S could exhibit a concentration gradient in the layer measured by the Auger technique. We solved this problem by comparing the AES results obtained on typical samples with those obtained on initially superstructure-free samples on which the $c(2 \times 2)$ was intentionally grown through S adsorption. In these experiments, a clean Ni surface was first produced by depositing a Ni layer *in situ* or selected among Ni tapes that had shown very low surface S content after the high temperature texturing anneal. Subsequently, a small amount of H_2S with a partial pressure of 5×10^{-7} – 1×10^{-6} torr was introduced in the vacuum chamber at a substrate temperature of 700–800 °C for few minutes and then pumped away. As known from several surface studies, the H_2S molecules dissociate at the Ni surface and S atoms chemisorb forming a $c(2 \times 2)$ superstructure with a coverage that saturates at 0.5 ML, corresponding to one complete atomic layer of the $c(2 \times 2)$ -S.^{11–13}

Exposures to H_2S as low as a few L [1 L (langmuir) $\equiv 10^{-6}$ torr s] produced very strong $c(2 \times 2)$ reflections in the RHEED patterns as shown in Fig. 6(a). The sulfur superstructure was stable at 800 °C after the H_2S was removed. CeO_2 and YSZ seed layers deposited *in situ* after S adsorption were highly oriented with a percentage of cube texture very close to 100%, as indicated by the (111) pole figure of Fig. 6(b). Longer exposure of the Ni surface to H_2S (≥ 1800 L) did not produce any degradation of the RHEED pattern that could be attributed to adsorption of surface S in excess of 0.5 ML¹⁴ or formation of a Ni sulfide phase. The as-grown superstructure was found to be stable also after exposure to air at room

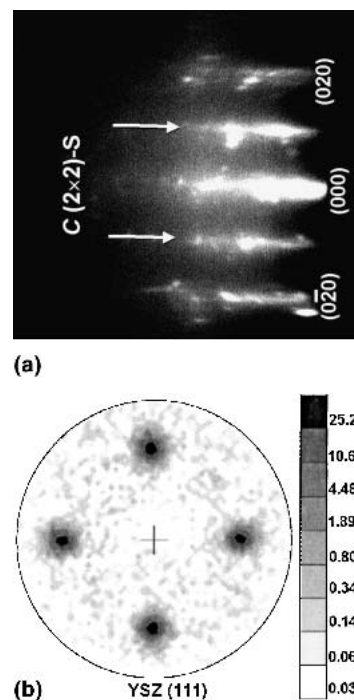


FIG. 6. (a) RHEED pattern showing strong $c(2 \times 2)$ reflections obtained after exposing a clean $\{100\}\langle 100\rangle$ Ni surface to few L of H_2S at 800 °C. (b) Logarithmic (111) pole figure of a YSZ seed layer grown *in situ* on the $c(2 \times 2)$ -S shown in (a). For this sample the x-ray background signal was eliminated by subtracting a second pole figure obtained after changing the Bragg angle by 1° . The calculated percentage of cube texture for this film was 99.96%.

temperature and consequent reheating of the sample in vacuum, which reproduced the same initial RHEED pattern. AES experiments performed *in situ* after S adsorption yielded a sulfur signal of about 25% at saturation.⁴ The same value was obtained on samples where the $c(2 \times 2)$ -S had formed consequent to segregation and showed RHEED patterns identical to the ones acquired in the S adsorption experiments. From these observations we associated an AES value of approximately 25% to a full layer of $c(2 \times 2)$ -S on the Ni surface. Consequently, we were able to quantify the S surface content in cases in which the superstructure did not cover the entire Ni surface and the $c(2 \times 2)$ reflections in the RHEED pattern were less intense than in fully covered samples.

Figure 7 shows a comparison of ϕ scans of the (111) peak for three different STO films grown on Ni samples showing (i) a complete $c(2 \times 2)$ layer, (ii) 40% of the full $c(2 \times 2)$ coverage, and (iii) no superstructure, respectively. We notice that an incomplete $c(2 \times 2)$ coverage is not sufficient to obtain a full cube texture of the seed layer, and in the case of 40% coverage, additional peaks indicating crystal domains grown with orientations other than cube on cube are still present in the ϕ scan. Figure 8 shows a similar comparison for two CeO_2 films deposited on two different Ni samples cut from the same tape but subjected to two different texturing anneals. In the

first case the sample was annealed in high vacuum at 1100 °C for 2 h and exhibited a complete S superstructure. In the second case the anneal was much longer (15 h) and caused partial evaporation of the surface S resulting in a weaker $c(2 \times 2)$ superstructure with about 70% coverage (see insets of Fig. 7). In both bases the Ni substrate showed a full width half-maximum (FWHM) of the (111) peak of $8.2^\circ \pm 0.4^\circ$. The CeO₂ films were cube textured and showed single (002) orientation on both the Ni substrates. However, it is evident that the degree of grain alignment for the CeO₂ films correlates with the coverage of the $c(2 \times 2)$ superstructure on the substrate, and the incomplete S template results in a broadening of the seed layer texture. We found that the texture of the seed layer replicates that of the substrate only when the $c(2 \times 2)$ has a full 0.5 ML coverage.

A sharpening in the cube texture of the seed layer corresponds to an enhancement in J_c of the YBCO film subsequently deposited on the completed (seed plus buffer layer) RABiT substrate. This relation is illustrated in Fig. 9, which plots the critical current density of four YBCO/CeO₂/YSZ/CeO₂/Ni samples versus the S surface content of the Ni substrate prior seed layer deposition. In this experiment, the different S coverage was obtained by

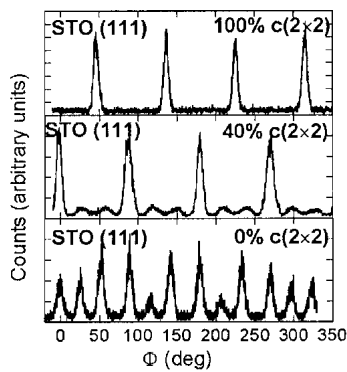


FIG. 7. Comparison between ϕ scans of the (111) peak for three different STO films grown on $\{100\}\langle 100\rangle$ Ni substrates having different sulfur coverage: 100% of a $c(2 \times 2)$ layer (or $\theta = 0.5$), top; 40%, middle; 0%, bottom.

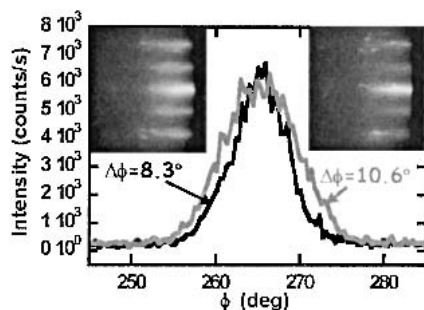


FIG. 8. ϕ scans of the (111) reflection of a CeO₂ seed layer grown on a Ni substrate annealed for 2 h (black line) and on a Ni substrate annealed for 15 h (gray line).

selecting a 1-m-long textured Ni tape showing only 40% of the S coverage corresponding to a full monolayer of $c(2 \times 2)$ and exposing it to H₂S in a subsequent anneal. In this case the texturing anneal, sulfurization, and seed layer (CeO₂) deposition were carried out *in situ* and continuously, in a reel-to-reel vacuum system equipped with an Auger spectrometer. The H₂S partial pressure was varied during the sulfurization treatment so that a different portion of the tape would show different S surface coverage at the end of the process. After deposition, four sections of the tape corresponding to four different S surface concentrations were cut, and YBCO was deposited on them by PLD.⁴

Sulfur adsorption experiments provide a method for quantifying the S coverage on the Ni surface after the texturing anneal. But, more importantly, H₂S exposure provides a rapid and efficient way to obtain a full coverage of the $c(2 \times 2)$ -S on textured Ni and, consequently, optimize the seed layer texture without being restricted by the amount of S actually present in the bulk and the slow, less efficient segregation process. H₂S exposure has been successfully introduced in a continuous process for texturing and CeO₂ coating of 1-m-long Ni tapes, yielding highly oriented and reproducible long lengths of RABiTS.⁴ YBCO films deposited on short sections of these RABiTS tapes by PLD and the *ex situ* BaF₂ method¹⁵ have consistently shown critical currents larger than 1 MA/cm².

In conclusion, we showed that the $c(2 \times 2)$ -S superstructure present on $\{100\}\langle 100\rangle$ Ni acts as a template that enables the epitaxial growth of oxide seed layers on the metal and that a complete coverage of this chemically stable layer is necessary to replicate the substrate texture in the buffer layer. Annealing the Ni substrate at 800 °C in the presence of a small amount of H₂S is sufficient to produce a stable $c(2 \times 2)$ -S with a coverage of 0.5 ML. This simple step allows creating a complete S template independently of the coverage obtained through segregation. Implementing this step in a continuous RABiTS fabrication process allows the initial Ni texturing anneal to be carried out at conditions that yield the

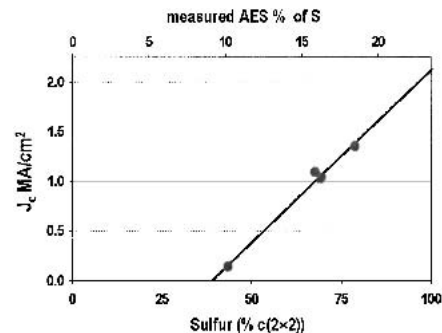


FIG. 9. Critical current density versus initial substrate S concentration for four YBCO/CeO₂/YSZ/CeO₂/Ni RABiTS samples.

best texture (and often involve high temperatures and consequent S evaporation) without being limited by the S segregation process.

ACKNOWLEDGMENT

Research was sponsored by the United States Department of Energy under Contract DE-AC05-00OR22725 with the Oak Ridge National Laboratory, managed by UT-Battelle, LLC.

REFERENCES

1. M. Paranthaman, A. Goyal, F.A. List, E.D. Specht, D.F. Lee, P.M. Martin, Qing He, D.K. Christen, D.P. Norton, J.D. Budai, and D.M. Kroeger, *Physica C* **275**, 266 (1997).
2. A. Goyal, R. Feenstra, F.A. List, M. Paranthaman, D.F. Lee, D.M. Kroeger, D.B. Beach, J.S. Morell, T.G. Chirayil, D.T. Verebelyi, X. Cui, E.D. Specht, D.K. Christen, and P.M. Martin, *JOM* **51**(7) (1999), p. 19.
3. Q. He, D.K. Christen, J.D. Budai, E.D. Specht, D.F. Lee, A. Goyal, D.P. Norton, M. Paranthaman, F.A. List, and D.M. Kroeger, *Physica C* **275**, 155 (1997).
4. M.M. Kowalewski, F.A. List, L. Heatherly, and D.M. Kroeger (unpublished); F.A. List, Continuous Processing of Coated Conductors, presented at the 2001 DOE Peer Review, Washington, DC (<http://www.ornl.gov/HTSC/fy01peer.htm>).
5. C. Cantoni, D.K. Christen, R. Feenstra, D.P. Norton, A. Goyal, G.W. Ownby, and D.M. Zehener, *Appl. Phys. Lett.* **79**, 3077 (2001).
6. M. Paranthaman, D.F. Lee, A. Goyal, E.D. Specht, P.M. Martin, X. Cui, J.E. Mathis, R. Feenstra, D.K. Christen, and D.M. Kroeger, *Supercond. Sci. Technol.* **12**, 319 (1999).
7. P.H. Holloway, *J. Vac. Sci. Technol.* **18**, 653 (1981).
8. S.S. Shoup, M.K. White, S.L. Krebs, N. Darnell, A.C. King, D.S. Mattox, I.H. Campbell, K.R. Marken, S. Hong, B. Czabaj, M.P. Paranthaman, H.M. Christen, H.Y. Zhai, and E. Specht, in *The Progress on Low-Cost, High-Quality, High-Temperature Superconducting Tapes Deposited by the Combustion Chemical Vapor Deposition Process*, edited by M.P. Paranthaman, M.W. Rupick, K. Salama, J. Mannhart, and T. Hasegawa (*Mater. Res. Soc. Symp. Proc.* **689**, 2001), p. 239.
9. P.C. McIntyre, *J. Appl. Phys.* **89**, 8074 (2001).
10. C. Cantoni, D.K. Christen, L. Heatherly, F.A. List, A. Goyal, G.W. Ownby, and D.M. Zehner, in *Proceedings of the 2002 American Ceramic Society Meeting* (American Ceramic Society, Westerville, OH, 2002).
11. M. Perdureau and J. Oudar, *Surf. Sci.* **20**, 80 (1970).
12. S. Andersson and J.B. Pendry, *J. Phys. C* **9**, 2721 (1976).
13. A. Patrige, G.J. Tatlock, F.M. Leibsle, and C.F.J. Flipse, *Phys. Rev. B* **48**, 8267 (1993).
14. C.A. Papageorgopoulos and M. Kamaratos, *Surf. Sci.* **338**, 77 (1995).
15. R. Feenstra, T.B. Lindemer, J.D. Budai, and M.D. Galloway, *J. Appl. Phys.* **69**(9), 6569 (1991).